Acta Crystallographica Section D
Biological Crystallography
ISSN 0907-4449

Structure of a highly stable mutant of human fibroblast growth factor 1

Anna Szlachcic,[a] Małgorzata Zakrzewska,[a] Daniel Krowarsch,[b] Vibeke Os,[c] Ronny Helland,[c] Arne O. Smalås[c] and Jacek Otlewski[a]*

[a]Department of Protein Engineering, Faculty of Biotechnology, University of Wroclaw, Wroclaw, Poland, [b]Department of Protein Biotechnology, Faculty of Biotechnology, University of Wroclaw, Wroclaw, Poland, and [c]The Norwegian Structural Biology Centre, Department of Chemistry, University of Tromsø, Tromsø, Norway

Correspondence e-mail: otlewski@protein.pl

Received 17 September 2008
Accepted 24 November 2008

PDB Reference: human fibroblast growth factor 1, Q40P/S47I/H93G mutant, 2q9x, r2q9xsf.

Fibroblast growth factors (FGFs) are involved in diverse cellular processes such as cell migration, angiogenesis, osteogenesis, wound healing and embryonic and foetal development. Human acidic fibroblast growth factor (FGF-1) is the only member of the FGF family that binds with high affinity to all four FGF receptors and thus is considered to be the human mitogen with the broadest specificity. However, pharmacological applications of FGF-1 are limited owing to its low stability. It has previously been reported that the introduction of single mutations can significantly improve the stability of FGF-1 and its resistance to proteolytic degradation. Here, the structure of the Q40P/S47I/H93G triple mutant of FGF-1, which exhibits much higher stability, a prolonged half-life and enhanced mitogenic activity, is presented. Compared with the wild-type structure, three localized conformational changes in the stable triple mutant were observed, which is in agreement with the perfect energetic additivity of the single mutations described in a previous study. The huge change in FGF-1 stability (the denaturation temperature increased by 21.5 K, equivalent to $\Delta\Delta G_{\rm den}$ = 24.3 kJ mol^{-1}) seems to result from the formation of a short 3_{10}-helix (position 40), an improvement in the propensity of amino acids to form β-sheets (position 47) and the rearrangement of a local hydrogen-bond network (positions 47 and 93).

1. Introduction

Fibroblast growth factors (FGFs) mediate diverse cellular responses in processes such as cell migration, angiogenesis, osteogenesis, wound healing, and embryonic and foetal development (Goldfarb, 1996). These growth factors bind to four different cell-membrane FGF receptors (FGFR1–4) which belong to the tyrosine kinase receptor family.

Human acidic fibroblast growth factor 1 (FGF-1) is a member of the fibroblast growth-factor family, which consists of 22 known polypeptide growth factors in mammals that share structural similarity and an affinity for heparin and/or heparan proteoglycans (Ornitz & Itoh, 2001; Powers *et al.*, 2000). FGFs range in molecular weight from 17 to 34 kDa and contain a highly conserved hydrophobic core formed by 12 antiparallel β-strands. In FGF-1 and FGF-2 these β-strands form a characteristic β-trefoil (Zhu *et al.*, 1991), which is one of the common protein superfolds (Orengo *et al.*, 1994) and is observed in proteins with diverse functions, such as Kunitz soybean trypsin inhibitors (Sweet *et al.*, 1974), interleukins 1α and 1β (Priestle *et al.*, 1989), hisactophilin (Habazettl *et al.*, 1992), ricin-like toxins (Tahirov *et al.*, 1995) and many others.

Such a fold can be divided into two parts, an 'upper' β-barrel and a 'lower' β-hairpin triplet, both of which are composed of six β-strands (Kim *et al.*, 2002). In FGF-1 the β-barrel is involved in binding to FGF receptors, while the β-hairpin triplet contains amino-acid residues that interact with heparin. FGF-1 is the only FGF that binds with high affinity to all four FGFRs and is considered to be the human mitogen with the broadest specificity (Chellaiah *et al.*, 1994).

The wide spectrum of biological activity of FGF-1 has triggered many attempts to develop its therapeutical application, such as in cardiovascular diseases (Post *et al.*, 2001; Sellke & Ruel, 2003), the improvement of endothelial healing after clinical angioplasty (Brewster *et al.*, 2006), stimulation of the neurogenic potential of astrocytes (Pillai *et al.*, 2006) and the delivery of anticancer chemotherapeuticals to tumour cells (Marcinkowska *et al.*, 2006). However, pharmacological applications of FGF-1 are limited owing to its low stability. Under physiological conditions, about 50% of wild-type FGF-1 molecules are unfolded as a consequence of its low denaturation temperature (Copeland *et al.*, 1991; Blaber *et al.*, 1999).

There have been several reports concerning improvement of the stability of FGF-1; most of these have been based on the introduction of point mutations into FGF-1, thus increasing its stability (Culajay *et al.*, 2000; Zakrzewska *et al.*, 2004, 2005; Dubey *et al.*, 2005; Lee *et al.*, 2006).

Here, we present the structure of the Q40P/S47I/H93G triple mutant of FGF-1 solved by X-ray crystallography to a resolution of 1.70 Å. Recently, we reported that this triple mutant of FGF-1 exhibits a significantly higher stability and an improved resistance to proteolytic degradation, which translates into a prolonged half-life and enhanced mitogenic activity. Moreover, the mitogenic activity of this mutant had risen nearly tenfold and its half-life was more than eightfold longer compared with that of wild-type FGF in the absence of heparin (Zakrzewska *et al.*, 2005).

2. Experimental procedures

2.1. Protein production and purification

The truncated 135-amino-acid form of wild-type FGF-1 (residues 6–140) cloned in the pET-3c plasmid was used for protein production and subsequent crystallization (Zakrzewska *et al.*, 2004). Q40P, S47I and H93G mutations were introduced using the QuikChange site-directed mutagenesis protocol (Stratagene) with mutagenic primers (Sigma). The introduced mutations were confirmed by DNA sequencing. The recombinant FGF-1 was expressed in the *Escherichia coli* BL21(DE3)pLysS host expression system (Invitrogen) and purified on heparin-Sepharose CL-6B and Superdex 75 HR 10/30 columns as described previously (Zakrzewska *et al.*, 2004; Wiedlocha *et al.*, 1996). The purity of the resulting protein was evaluated by SDS–PAGE and the presence of mutations was confirmed by electrospray ionization mass spectrometry. The protein concentrations were determined spectrophotometrically using molar extinction coefficients as described by Pace *et al.* (1995).

2.2. Chemical denaturation

Chemical denaturation was monitored using fluorescence spectroscopy. Measurements were carried out at a protein concentration of 1.2×10^{-6} *M* in a 10 mm cuvette using a FP-750 spectrofluorimeter (Jasco) equipped with an ETC 272T Peltier accessory with an excitation wavelength of 280 nm. FGF-1 denaturation could be monitored by the changes in fluorescence emission intensity at 353 nm characteristic of the single Trp107. Chemical denaturation was performed by incubating the protein in various concentrations of guanidinium chloride (GdmCl) in 25 m*M* phosphate buffer pH 7.3 at 294.15 K for 24 h. The concentration of GdmCl in the individual samples was determined refractometrically (Nozaki, 1972).

Denaturation data were fitted assuming a two-state reversible equilibrium transition (Blaber *et al.*, 1999) and the apparent free-energy change in the absence of GdmCl (ΔG) was determined by the fitting the fluorescence intensity changes at a particular concentration of GdmCl to the equation given by Santoro & Bolen (1992) using *PeakFit* (Jandel Scientific Software).

2.3. Crystallization

The purified FGF-1 mutant was equilibrated in 25 m*M* Na_2HPO_4, 100 m*M* NaCl, 10 m*M* ammonium sulfate, 1 m*M* EDTA pH 7.3 and concentrated to 8–10 mg ml^{-1} using a Centricon-10 spin concentrator (Amicon). The homogeneity of the concentrated protein sample at various temperatures was tested using DLS (dynamic light scattering). Measurements were carried out on a DynaPro DLS (Wyatt) at 5 K intervals from 277 to 312 K. A temperature of 293 K was chosen for crystallization trials as the polydispersity of the sample was lowest at this temperature.

Crystallization was performed using the hanging-drop vapour-diffusion method. Initial screens (Hampton Research Crystal Screens I and II and Index Screen) yielded several conditions containing crystals, which were then optimized. Crystals suitable for X-ray diffraction studies grew in approximately 5–7 d at 293 K in 2 µl drops equilibrated against 600 µl reservoir solution containing 15% PEG 8000 and 100 m*M* Tris–HCl pH 7.5. Crystals were soaked in reservoir solution containing 20% glycerol before being flash-frozen in liquid nitrogen.

2.4. Data collection, structure determination and refinement

Diffraction data were collected to 1.70 Å resolution on the Swiss–Norwegian beamlines (BM01) at the European Synchrotron Radiation Facility (ESRF, Grenoble, France). The data were indexed and integrated using *MOSFLM* (Leslie, 1992). Scaling and merging of the data and subsequent conversion of intensities into structure factors were performed using the *CCP*4 programs *SCALA* and *TRUNCATE* (Collaborative Computational Project, Number 4, 1994). The structure of the stable FGF-1 triple mutant was solved by molecular replacement using *MOLREP* (Collaborative Computational Project, Number 4, 1994; Vagin & Teplyakov,

1997). The search model was based on the 1.10 Å resolution structure of wild-type FGF-1 (PDB code 1rg8; Bernett *et al.*, 2004).

After automatic model building with *ARP/wARP* (Perrakis *et al.*, 1999), 123 of the 135 amino-acid residues were initially placed into the electron density. The $2F_o - F_c$ and $F_o - F_c$ electron-density maps were calculated and manual model building was carried out using the graphics program *O* (Jones *et al.*, 1991). Further refinement was performed using *REFMAC*5 (Murshudov *et al.*, 1997) within the *CCP*4 program suite (Collaborative Computational Project, Number 4, 1994). Solvent molecules were added if the corresponding $F_o - F_c$ peaks were higher than 3σ and their *B* factors were lower than 30 Å^2. 5% of the data were selected randomly for cross-validation purposes in subsequent steps and were not used in refinement (Brünger, 1992).

3. Results and discussion

The Q40P/S47I/H93G triple mutant of FGF-1 exhibits significantly increased stability. The introduction of these three substitutions leads to a 21.5 K increase in the denaturation temperature of the protein, which is much more resistant to proteolytic degradation (Zakrzewska *et al.*, 2005). Two of these mutations (Q40P and S47I) were designed and tested in our laboratory and the third (H93G) has been described by Blaber and coworkers (Culajay *et al.*, 2000).

We found perfect additivity of the single-mutation stabilities when combined in the multiple mutant, which suggests that the substitutions cause independent energetic effects in different regions of the FGF-1 structure (Zakrzewska *et al.*, 2005). Our aim was to determine the crystal structure of the FGF-1 triple mutant and to analyze the structural changes that influence the thermodynamic properties of the protein.

3.1. Chemical denaturation

We previously determined the thermal stabilities of wild-type FGF-1 and its triple mutant in 25 m*M* sodium phosphate pH 7.3 buffer containing 0.7 *M* GdmCl in order to avoid protein aggregation (Zakrzewska *et al.*, 2005). In order to directly compare the stabilities of the proteins, we now performed chemical denaturation with GdmCl. Chemical denaturation curves of the triple mutant and the wild type are shown in Fig. 1. The data enable the calculation of the stability parameters *m*, $GdmCl_{1/2}$ and ΔG. The *m* value, which is a measure of the cooperativity of the unfolding transition, for the triple mutant is 19.2 kJ mol^{-1} M^{-1} and is very similar to the value for the wild type (20.4 kJ mol^{-1} M^{-1}). The GdmCl concentration at the mid-point of transition ($GdmCl_{1/2}$), which shows the change in resistance to chemical denaturation, is 2.11 *M* for the mutant, compared with 1.13 *M* for the wild type (Zakrzewska *et al.*, 2004). The data indicate that the introduction of three stabilizing mutations results in a ΔG (free-energy change of denaturation in the absence of denaturant, stabilization energy) of 40.9 kJ mol^{-1}, *i.e.* 17.7 kJ mol^{-1} greater than that of the wild type. The results obtained from chemical denaturation show good agreement with the thermal denaturation data (the stability increase was equal to 24.2 kJ mol^{-1}; Zakrzewska *et al.*, 2005).

3.2. The crystal structure determination

The crystal structure of the Q40P/S47I/H93G triple mutant of FGF-1 was solved at 1.70 Å resolution using molecular replacement with wild-type FGF-1 as a search model (Bernett *et al.*, 2004). The crystal used for data collection was approximately 200 × 40 × 30 µm in size, with rod-like morphology (Fig. 2). The space group was identified as orthorhombic $P2_12_12_1$, with unit-cell parameters a = 34.61, b = 57.60, c = 57.72 Å, $\alpha = \beta = \gamma = 90^\circ$ and one molecule in the asymmetric unit. Data were collected with an overall completeness of 100%. The final structure, which consisted of residues 6–136 and 107 solvent molecules, has been refined to R_{work} and R_{free} values of 20.75% and 24.47%, respectively. Data-collection, refinement and model statistics are given in Table 1.

After automatic model building with *ARP/wARP*, the electron density in the region of the H93G mutation (residues

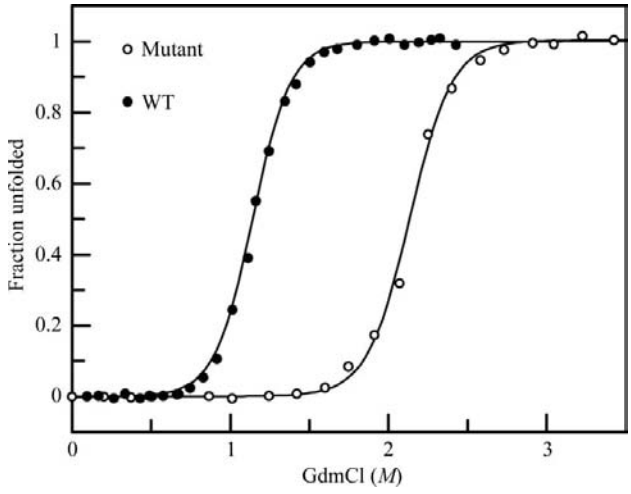

Figure 1
Normalized chemical denaturation curves of wild-type FGF-1 and the stable triple mutant monitored by changes in fluorescence at 353 nm.

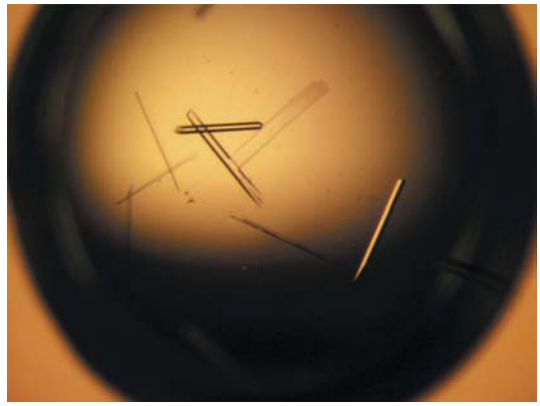

Figure 2
FGF-1 triple-mutant crystals.

Table 1
Data-collection and refinement summary.

Values in parentheses are for the outer shell.

Data-collection statistics	
Beamline	Swiss–Norwegian beamlines (BM01)
Detector	MAR CCD
Wavelength (Å)	0.86980
Space group	$P2_12_12_1$
Unit-cell parameters	
a (Å)	34.61
b (Å)	57.60
c (Å)	57.72
Resolution range (Å)	34.6–1.70 (1.79–1.70)
$R_{\rm merge}$ (%)	9.7 (35.6)
Multiplicity	4.0 (4.0)
$I/\sigma(I)$	5.2 (1.9)
Mean $I/\sigma(I)$	10.1 (3.4)
Completeness (%)	100.0 (100.0)
Wilson B factor (Å^2)	11.93
Refinement statistics	
No. of atoms	1119
B factor (Å^2)	10.69
$R_{\rm free}$ (%)	24.47
$R_{\rm work}$ (%)	20.75
Geometrical deviation	
Bonds (Å)	0.015
Angles (°)	1.533
ESU (Å)	0.13
Ramachandran plot, residues in	
Most favoured regions (%)	94.3
Additionally allowed regions (%)	4.7
Disallowed regions (%)	0.0

90–93) was very poorly defined and not even the backbone of these four amino acids could be placed in the density map. Manual model building and refinement improved the electron density in this region and the positions of the backbone atoms could be determined. Further refinement also allowed the definition of the positions of the side-chains atoms of residues 90 and 93.

No electron density was observed for the first five and the last three amino-acid residues of the FGF-1 mutant molecule.

PROCHECK analysis (Laskowski *et al.*, 1993) based on the final refined PDB file was performed using the EBI server (http://www.ebi.ac.uk). On the basis of the resulting Ramachandran plot, 100 residues (94.3%) were in the most favoured regions (only considering nonglycine and nonproline residues), five residues (4.7%) were in additional allowed regions and one was in the generously allowed region. The φ–ψ angles of individual residue types are also located in allowed regions of Ramachandran plots for individual residue types, as well as the χ_1–χ_2 angles. The G factors for both dihedral angles and bond lengths fitted well into the proper range of values and no bad molecular contacts were found by *PROCHECK*. Thus, we conclude that the final model is geometrically and stereochemically correct.

3.3. Structural comparison to wild-type FGF-1

In the structural analysis of the stable Q40P/S47I/H93G mutant, we compared its conformation with the best available structure of the wild type (PDB code 1rg8; Bernett *et al.*, 2004). The C$^\alpha$ r.m.s.d. between the triple-mutant structure and the wild-type FGF-1 structure was 0.68 Å. Compared with the wild type, we only observed local differences within the Q40P/S47I/H93G mutant structure; no global conformational changes were seen. This observation is in agreement with the energetic additivity of single mutations described in our previous study (Zakrzewska *et al.*, 2005). The major structural differences are localized in the loop between residues Leu89 and Asn95 (the region of the H93G mutation); less significant differences were found within residues Thr34–Ile42 (the surroundings of the Q40P mutation) and the smallest changes were observed in β-strand 4 (in the proximity of the S47I mutation) (Fig. 3). The largest C$^\alpha$ r.m.s.d. between the triple-mutant structure and the wild type within regions containing mutations is 2.01 Å close to the H93G mutation; the smallest, in the S47I mutation region, is 0.40 Å.

The Q40P mutation is located within a turn between strands β3 and β4. Structural analysis of the wild-type structure (PDB code 1rg8) using *PROCHECK* revealed a type I β-turn between residues 39 and 42. According to statistical analysis (Hutchinson & Thornton, 1994), proline is the most favoured residue at position i + 1 of a type I β-turn (4.3 times more common than glutamine, which is in position 40 in the wild type). The large increase in protein stability observed for the single Q40P mutant of FGF-1 (almost an 8 K increase in denaturation temperature, 7.5 kJ mol^{-1}; Zakrzewska *et al.*, 2005) may indicate that the introduction of proline produces improved conformational adjustments and that the type I β-turn should be preserved within the triple-mutant structure. However, structural analysis of the triple mutant revealed a slight change in the local backbone conformation within the region Thr34–Ile42 (compared with the wild type). Using *PROCHECK* for secondary-structure analysis, we did not find a β-turn in the close proximity of residue 40, but a three-amino-acid 3_{10}-helix (Pro40–Ile42). Short 3_{10}-helices exhibit strong amino-acid preferences and proline is a highly over-represented residue at the first position in such structures (Karpen *et al.*, 1992; Pal *et al.*, 2003). A similar conformation is observed in the structure of a close structural homologue of FGF-1, basic fibroblast growth factor (FGF-2). The proline residue occurring at position 49 in FGF-2 (corresponding to position 40 in FGF-1) is the first residue of 3_{10}-helix, Pro49–Ile51 (Eriksson *et al.*, 1993), and the polypeptide chains of FGF-2 and the triple mutant adopt almost identical conformations within this region.

The three-amino-acid 3_{10}-helix found in the triple mutant can be considered as two consecutive overlapping type I β-turns: the first comprising residues Asp39–Ile42 and the second comprising residues Pro40–Gln43, with two consecutive 4$\rightarrow$1 hydrogen bonds between the carbonyl O atom at position i and the amide H atom at position i + 3 (Karpen *et al.*, 1992; Pal *et al.*, 2003).

In addition, Pro mutants are expected to stabilize proteins by decreasing the conformational entropy of the denatured state: the pyrrolidine ring of proline restricts this residue to fewer conformations than are available to other amino acids (Matthews *et al.*, 1987; Choi & Mayo, 2006). Since the structural changes caused by the Q40P mutation are modest, in the

case of FGF-1 this factor may be a significant contribution to the observed stability gain.

The stabilizing effect of the Q40P mutation can thus be explained by the change in the energetics of the denatured state combined with the improved amino-acid propensity. The short 3_{10}-helix present in the mutant structure can be considered as two overlapping β-turns, with similar geometry as the type I β-turn in the wild-type structure. Proline is the most favoured residue at position 40 in both the type I β-turn and the three-amino-acid 3_{10}-helix.

The S47I mutation, which provides the greatest increase in denaturation temperature (9.0 K, 9.2 kJ mol^{-1}) of the single FGF-1 mutants, is located in the middle of β-strand 4. Surprisingly, this substitution results in small conformational changes (Fig. 3*c*). Since the structural changes are minimal (the largest r.m.s.d. for C^{α} atoms between the mutant and the wild type in the proximity of the S47I mutation is 0.40 Å), the strong stabilizing effect of the mutation may originate from the secondary-structure propensities and rearrangement of the hydrogen-bond network.

According to statistical scales of β-sheet propensities (Chou & Fasman, 1978; Kim & Berg, 1993; Minor & Kim, 1994*a*,*b*; Smith *et al.*, 1994; Kallberg *et al.*, 2001), isoleucine is favoured over serine by almost twofold in the formation of a β-sheet. Analysis of the main-chain dihedral angles shows that an isoleucine at position 47 adopts dihedral angle values that are located in the centre of the most favoured region *B* of the Ramachandran plot ($\varphi = -113^{\circ}$ and $\psi = 124^{\circ}$), while in the wild-type structure they are found much closer to the border of this region ($\varphi = -149^{\circ}$ and -143° and $\psi = 145^{\circ}$ and 150°, depending on the molecule in the crystal asymmetric unit).

The range of free-energy differences observed between the best and the worst β-sheet-forming residues (excluding Pro) varies in the different β-sheet propensity scales [from approximately 2.1 kJ mol^{-1} in the zinc-finger study by Kim & Berg (1993) to 11.7 kJ mol^{-1} for the protein G IgG-binding domain as determined by Smith *et al.* (1994)]. The respective range for the free-energy change for a Ser to Ile mutation is between 0.71 and 1.59 kJ mol^{-1}. These differences can be explained by the fact that β-sheet propensity is strongly modulated by its tertiary context. However, the observed stability gain appears to be too high considering only improvement of β-sheet propensity.

Additionally, we observe a rather complex rearrangement of hydrogen bonds and van der Waals interactions in the vicinity of the S47I substitution. The hydrogen bonds between the main chain of Ile47 and the main chain of Tyr55 are shortened by around 0.15 Å in the triple mutant compared with the wild-type structure. In the wild-type structure, the side chain of Ser47 is involved in water-mediated hydrogen bonds to the main chain of Gln45 and the main chain of Ala48, whereas in the region of the S47I mutation several van der Waals interactions (Leu44 with the side chain of Gln45, Ser50 and Leu84 with the side chain of Glu49) are gained. In the triple-mutant structure, we did not observe the 2.8 Å hydrogen bond between the side chains of Gln45 and Lys57 that is present in the wild-type structure. However, this hydrogen bond is located on the surface of the growth-factor molecule. Such solvent-exposed hydrogen bonds do not generally contribute significantly to the overall protein stability (Horovitz *et al.*, 1990).

In conclusion, the likely origin of the stability gain arising from the S47I mutation is a combination of convergent effects of improved β-sheet propensity, improved main-chain dihedral angles and new van der Waals interactions.

The largest structural rearrangement (compared with the wild type) was observed within the region of the H93G mutation (Fig. 3*d*). The conformation and stability of the H93G mutant have been analyzed by Blaber and coworkers (Kim *et al.*, 2002). Residues 90–93 form a type I β-turn, with glycine 93 at the $i + 3$ position, which is located in the left-handed α-helical region of the Ramachandran plot. The location of nonglycine residues in this region (such as histidine in wild-type FGF-1) cause steric strain between the backbone atoms and side-chain C^{β} atoms (Kimura

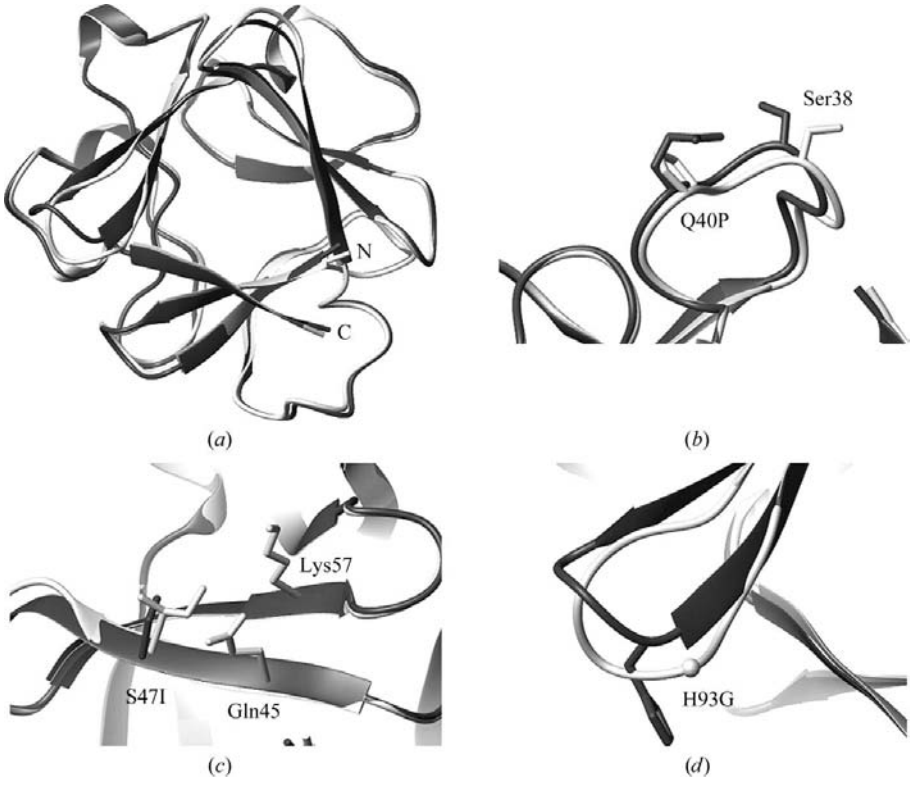

Figure 3
(*a*) Superposition of wild-type FGF-1 (PDB code 1rg8) and the Q40P/S47I/H93G mutant (PDB code 2q9x). Regions of mutated residues are shown in (*b*) (Q40P), (*c*) (S47I) and (*d*) (H93G). The wild-type structure is shown in dark grey and that of the triple mutant in light grey.

et al., 1992; Stites *et al.*, 1994; Takano *et al.*, 2001). It has been reported that the mutation of such a strained residue to glycine can increase the thermal stability of the protein, especially if the introduced glycine residue is located at the $i + 3$ position in a type 3:5 or 4:6 β-hairpin turn (Kim *et al.*, 2003). Therefore, the large 7.3 K (Culajay *et al.*, 2000) increase in protein stability is likely to originate from the elimination of the conformational strain resulting from the interaction of the His93 side chain with its main-chain carbonyl group.

A slight hydrogen-bonding network rearrangement was also observed: the hydrogen bond between the side chain of Glu90 and the hydroxyl group of Tyr125 was not observed in the triple mutant. Instead, an ionic interaction was found between the Glu90 side chain and the guanidyl group of Arg88 and a hydrogen bond was identified between the side chains of Asp95 and Tyr97.

Surprisingly, we found structural differences from the triple-mutant β-turn conformation in both the wild-type and H93G (PDB code 1k5u; Kim *et al.*, 2002) structures (Fig. 3*d*). These structural differences can be partly explained by the fact that the resolution and completeness of the data collected for the triple mutant were higher than in the case of the single H93G mutant (1k5u; 2.0 Å and 78%, respectively).

In summary, we observed three localized conformational changes in the highly stable triple mutant compared with the wild-type structure. The 21.5 K increase in FGF-1 stability is likely to result from a decrease in the conformational entropy of the denatured state on the introduction of a proline residue and a slight rearrangement of the β-turn geometry to form a short 3_{10}-helix (position 40), coinciding with the effects of improved β-sheet propensity and increased van der Waals interactions (position 47) and the release of steric strain of a histidine residue in a left-handed helical conformation together with rearrangement of the local hydrogen-bond network (position 93).

This work was supported by the Polish Ministry of Science and higher Education (grant no. N N301 4192 33). Provision of beamtime at the Swiss–Norwegian Beamlines (SNBL, BM01) at the European Synchrotron Radiation Facility (ESRF) is gratefully acknowledged. The Norwegian Structural Biology Centre (NorStruct) is funded by the University of Tromsø and by the Functional Genomics (FUGE) initiative of the Research Council of Norway.

References

Bernett, M. J., Somasundaram, T. & Blaber, M. (2004). *Proteins*, **57**, 626–634.
Blaber, S. I., Culajay, J. F., Khurana, A. & Blaber, M. (1999). *Biophys. J.* **77**, 470–477.
Brewster, L., Brey, E. M., Addis, M., Xue, L., Husak, V., Ellinger, J., Haudenschild, C. C. & Greisler, H. P. (2006). *Am. J. Surg.* **192**, 589–593.
Brünger, A. T. (1992). *Nature (London)*, **355**, 472–475.
Chellaiah, A. T., McEwen, D. G., Werner, S., Xu, J. & Ornitz, D. M. (1994). *J. Biol. Chem.* **269**, 11620–11627.
Choi, E. J. & Mayo, S. L. (2006). *Protein Eng. Des. Sel.* **19**, 285–289.
Chou, P. Y. & Fasman, G. D. (1978). *Adv. Enzymol. Relat. Areas Mol. Biol.* **47**, 45–148.
Collaborative Computational Project, Number 4 (1994). *Acta Cryst.* D**50**, 760–763.
Copeland, R. A., Ji, H., Halfpenny, A. J., Williams, R. W., Thompson, K. C., Herber, W. K., Thomas, K. A., Bruner, M. W., Ryan, J. A., Marquis-Omer, D., Sanyal, G., Sitrin, R. D., Yamazaki, S. & Middaugh, C. R. (1991). *Arch. Biochem. Biophys.* **289**, 53–61.
Culajay, J. F., Blaber, S. I., Khurana, A. & Blaber, M. (2000). *Biochemistry*, **39**, 7153–7158.
Dubey, V. K., Lee, J. & Blaber, M. (2005). *Protein Sci.* **14**, 2315–2323.
Eriksson, A. E., Cousens, L. S. & Matthews, B. W. (1993). *Protein Sci.* **2**, 1274–1284.
Goldfarb, M. (1996). *Cytokine Growth Factor Rev.* **7**, 311–325.
Habazettl, J., Gondol, D., Wiltscheck, R., Otlewski, J., Schleicher, M. & Holak, T. A. (1992). *Nature (London)*, **359**, 855–858.
Horovitz, A., Serrano, L., Avron, B., Bycroft, M. & Fersht, A. R. (1990). *J. Mol. Biol.* **216**, 1031–1044.
Hutchinson, E. G. & Thornton, J. M. (1994). *Protein Sci.* **3**, 2207–2216.
Jones, T. A., Zou, J.-Y., Cowan, S. W. & Kjeldgaard, M. (1991). *Acta Cryst.* A**47**, 110–119.
Kallberg, Y., Gustafsson, M., Persson, B., Thyberg, J. & Johansson, J. (2001). *J. Biol. Chem.* **276**, 12945–12950.
Karpen, M. E., De Haseth, P. L. & Neet, K. E. (1992). *Protein Sci.* **1**, 1333–1342.
Kim, C. A. & Berg, J. M. (1993). *Nature (London)*, **362**, 267–270.
Kim, J., Blaber, S. I. & Blaber, M. (2002). *Protein Sci.* **11**, 459–466.
Kim, J., Brych, S. R., Lee, J., Logan, T. M. & Blaber, M. (2003). *J. Mol. Biol.* **328**, 951–961.
Kimura, S., Kanaya, S. & Nakamura, H. (1992). *J. Biol. Chem.* **267**, 22014–22017.
Laskowski, R. A., MacArthur, M. W., Moss, D. S. & Thornton, J. M. (1993). *J. Appl. Cryst.* **26**, 283–291.
Lee, J., Dubey, V. K., Somasundaram, T. & Blaber, M. (2006). *Proteins*, **62**, 686–697.
Leslie, A. G. W. (1992). *Jnt CCP4/ESF–EACBM Newsl. Protein Crystallogr.* **26**.
Marcinkowska, E., Superat, K. & Wiedlocha, A. (2006). *Oncol. Res.* **16**, 27–34.
Matthews, B. W., Nicholson, H. & Becktel, J. (1987). *Proc. Natl Acad. Sci. USA*, **84**, 6663–6667.
Minor, D. L. Jr & Kim, P. S. (1994*a*). *Nature (London)*, **367**, 660–663.
Minor, D. L. Jr & Kim, P. S. (1994*b*). *Nature (London)*, **371**, 264–267.
Murshudov, G. N., Vagin, A. A. & Dodson, E. J. (1997). *Acta Cryst.* D**53**, 240–255.
Nozaki, Y. (1972). *Methods Enzymol.* **26**, 43–50.
Orengo, C. A., Jones, D. T. & Thornton, J. M. (1994). *Nature (London)*, **372**, 631–634.
Ornitz, D. M. & Itoh, N. (2001). *Genome Biol.* **2**, 1–12.
Pace, C. N., Vajdos, F., Fee, L., Grimsley, G. & Gray, T. (1995). *Protein Sci.* **4**, 2411–2423.
Pal, L., Chakrabarti, P. & Basu, G. (2003). *J. Mol. Biol.* **326**, 273–291.
Perrakis, A., Morris, R. & Lamzin, V. S. (1999). *Nature Struct. Biol.* **6**, 458–463.
Pillai, R., Scintu, F., Scorciapino, L., Carta, M., Murru, L., Biggio, G., Cabras, S., Reali, C. & Sogos, V. (2006). *Exp. Cell Res.* **312**, 2336–2346.
Post, M. J., Laham, R., Sellke, F. W. & Simmons, M. (2001). *Cardiovasc. Res.* **49**, 522–531.
Powers, C. J., McLeskey, S. W. & Wellstein, A. (2000). *Endocr. Relat. Cancer*, **7**, 165–197.
Priestle, J. P., Schar, H. P. & Grütter, M. G. (1989). *Proc. Natl Acad. Sci. USA*, **86**, 9667–9671.
Santoro, M. M. & Bolen, D. W. (1992). *Biochemistry*, **31**, 4901–4907.
Sellke, F. W. & Ruel, M. (2003). *Ann. Thorac. Surg.* **75**, S685–S690.
Smith, C. K., Withka, J. M. & Regan, L. (1994). *Biochemistry*, **33**, 5510–5517.

Stites, W. E., Meeker, A. K. & Shortle, D. (1994). *J. Mol. Biol.* **235**, 27–32.
Sweet, R. M., Wright, H. T., Janin, J., Chothia, C. H. & Blow, D. M. (1974). *Biochemistry*, **13**, 4212–4228.
Tahirov, T. H., Lu, T. H., Liaw, Y. C., Chen, Y. L. & Lin, J. Y. (1995). *J. Mol. Biol.* **250**, 354–367.
Takano, K., Yamagata, Y. & Yutani, K. (2001). *Proteins*, **45**, 274–280.
Vagin, A. & Teplyakov, A. (1997). *J. Appl. Cryst.* **30**, 1022–1025.
Wiedlocha, A., Falnes, P. O., Rapak, A., Munoz, R., Klingenberg, O. & Olsnes, S. (1996). *Mol. Cell. Biol.* **16**, 270–280.
Zakrzewska, M., Krowarsch, D., Wiedlocha, A., Olsnes, S. & Otlewski, J. (2005). *J. Mol. Biol.* **352**, 860–875.
Zakrzewska, M., Krowarsch, D., Wiedlocha, A. & Otlewski, J. (2004). *Protein Eng. Des. Sel.* **17**, 603–611.
Zhu, X., Komiya, H., Chirino, A., Faham, S., Fox, G. M., Arakawa, T., Hsu, B. T. & Rees, D. C. (1991). *Science*, **251**, 90–93.